crystals

MDPI

Supplementary materials

Fast Tunable Biological Fluorescence Detection Device with Integrable Liquid Crystal Filter

Qing Yang [1], Tong Sun [1,2], Xinyu Wu [1,2], Guangchao Cui [1,2], Mengzheng Yang [1,2], Zhongyang Bai [1,2], Lin Wang [2], Helin Li [1,2], Wenjing Chen [2], Qunwen Leng [1,2], Robert Puers [4], Ceyssens Frederik [4], Michael Kraft [4], Qinglin Song [5], Huabin Fang [5], Dewen Tian [5], Dexin Wang [5], Huijie Zhao [3,6], Weisheng Zhao [1,2], Tianxiao Nie [1], Qi Guo [3,*] and Lianggong Wen [1,2,*]

[1] School of Integrated Circuit Science and Engineering, Beihang University, Beijing, 100191, China; zy1702517@buaa.edu.cn (Q.Y.); suntong@buaa.edu.cn (T.S.); zy1702515@buaa.edu.cn (X.W.); zy1702502@buaa.edu.cn (G.C.); yangmengzheng@buaa.edu.cn (M.Y.); baizhongyang@buaa.edu.cn (Z.B.); lihelin618@buaa.edu.cn (H.L.); lengqw@bhqditi.com (Q.L.); weisheng.zhao@buaa.edu.cn (W.Z.); nietianxiao@buaa.edu.cn (T.N.)

[2] Beihang-Goertek Joint Microelectronics Institute, Qingdao Research Institude, Qingdao, 266101, China; wangl@bhqditi.com (L.W.); chenwj@bhqditi.com (W.C.);

[3] School of Instrumentation and Optoelectronic Engineering, Beihang University, Beijing 100191, China; hjzhao@buaa.edu.cn (H.Z.)

[4] ESAT-MICAS, KU Leuven, Kasteelpark Arenberg 10, 3001 Leuven, Belgium; bob.puers@esat.kuleuven.be (R.P.); Frederik.Ceyssens@esat.kuleuven.be (C.F.); michael.kraft@kuleuven.be (M.K.)

[5] Qingdao Goertek Microelectronics Research Institute Co., Ltd., Qingdao 266104, China; kelen.song@goermicro.com (Q.S.); robin.fang@goermicro.com (H.F.); Rico.tian@goermicro.com (D.T.); dexin.wang@goermicro.com (D.W.)

[6] Beihang University Qingdao Research Institute, Qingdao, 266101, China;

* Correspondence: qguo@buaa.edu.cn (Q.G.); wenlg@buaa.edu.cn (L.W.)

Table S1. The diameters of some typical cells.

	MCF-7	KATO III	PC-3	Leukocyte
Diameter (μm)	6–17	5–13	5–15	6–20

Table S2. Summary of bio-fluorescence detection techniques.

Features	Flow Cytometer [1]	Microscope [2]	Confocal [3]	This work
Transmittance	~40%	~90%	~60%	~80%
Resolution	~250 μm	~2.8 μm	~0.14 μm	~6 μm
Responding Speed	Fast	Slow	Fast	Fast
Continuous Observation	No	Yes	Yes	Yes
Convenience	Yes	Yes	No	Yes
High Flow Detection	Yes	No	No	Yes
Cost	~$70,000	~$5000	~$300000	~$5000

According to the Table S2, the device with LCTF for bio-fluorescence detection can meet the both requirement of continuous observation and high flow detection with high transmittance and resolution. The fast responding speed guarantee the accuracy of rapid detection of various biological samples. Compared to other techniques, the device with LCTF for bio-fluorescence detection has greater potential in achieving a miniaturized, multipurpose and fast detection platform with high sensitivity and low power consumption.

Table S3. Some comparisons of the liquid crystal tunable filter for bio-detection.

Features	This work	Lee. J. H, et. al [4]	Behrooz. A, et. al [5]	Lee. O, et. al [6]
Sample	Cell/ Bacteria	Cell	Tumor	Fibroblasts
Responding Speed	~20 ms	≤1 s	≤1 s	≤1 s
Integration	High	High	Low	Medium
DistanceΔf	59 nm	2.2 nm	10 nm	10 nm
Cost	Low	High	High	Low

DistanceΔf of the Table S3 is defined as the minimum wavelength difference between any two fluorescence channels in all fluorescence spectra, as shown in Equation S (1).

$$\Delta f = min\lfloor f_m - f_n \rfloor \quad \text{(S1)}$$

In order to prepare a shadow mask pattern, a lift-off process was used in preparation of the shadow mask for the biological material culture, as Figure S1. (a) illustrates. AZ5214 and LOR (MicorChem lift-off resists) were used for the lift-off-technique. LOR was coated thinly (about 1 μm) on a glass die with a spin-coating process. After coating and soft baking, a SUSS MicroTec MA6 mask aligner was used as a lithography tool for the patterning. Vapor deposition of titanium metal was carried out by electron beam evaporation technology. The speed was about 10 Å/s, and the thickness spec of the metal layer was 120 nm. Eventually sacrificial releasing was conducted to complete the lift off shadow mask preparation in the Aceton bath of density 99.5%.

In the process of cell cultivation, Hela cells were labeled with green and red fluorescent proteins for the experiments. First, the patterned shadow mask was placed into the cultivation bottle after an alcohol treatment. Then, 4 ml of the cell cultivation suspension liquid was injected into the bottle. The bottle was then sealed and put into the cell cultivation environment at 35 °C with 5% CO_2 and 95% air. After the cells adhered to the plate, the shadow mask preparation was completed and ready for the consequent fluorescence detection experiments. The process is shown in Figure S1b.

As for the cultivation process of the Pseudomonas, unlike the cell culture, Pseudomonas requires a solid media, as shown in Figure S1c. Firstly, a Ti-coated shadow mask after a liquid crystal treatment was put into the cultivation bottle, and then the prepared cultivation medium was applied into it. After a duration of two hours until the culture medium was fixed, a small amount of Pseudomonas fluorescents was scratched out with the inoculation ring and applied on the culture medium by a scribe method. The cultivation bottle was then sealed and cooled down to 4 °C. When the pseudomonas were formed, the glass plate was taken out and the surface colonies were illuminated by excitation light to stimulate the fluorescence emission by the bacteria.

Considering that the growth conditions of Pseudomonas and Hela cells are different, and co-culture is not easy to control the sample density during observation, the three samples have been cultivated separately under the most suitable growth conditions.

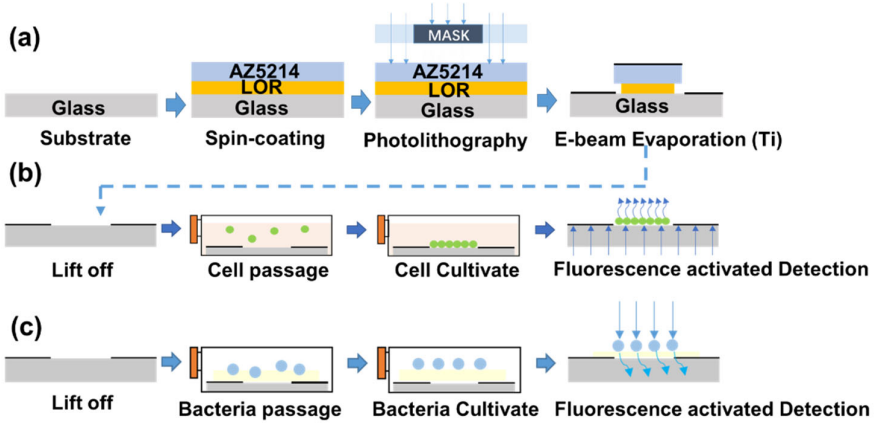

Figure S1. Pattern production and cells cultivation: (**a**) Shadow mask patterning process; (**b**) Cell cultivation process; (**c**) Pseudomonas cultivation process.

According to reference [7] in supplementary material, a simple numerical analysis of Equation (4) in the paper will be expanded in this section. By introducing Equation (4), the relationship of transmittance at different wavelengths can be calculated as: G (509 nm) > B (450 nm) > R (610nm). Similarly, the result of transmittance-R (610nm) > G (509 nm) > B (450 nm) can also be obtained at 1.9V.

Reference:

1. Han, Y.; Gu, Y.; Zhang, A.C.; Lo, Y. H. Imaging technologies for flow cytometry. *Lab on a Chip*, **2016**, *16(24)*, 4639-4647.
2. Wang, B.; Lin, Q.; Shen, C.; Han, Y.; Tang, J.; Chen, H. Synthesis of MA POSS–PMMA as an intraocular lens material with high light transmittance and good cytocompatibility. *Rsc Advances*, **2014**, *4(95)*, 52959-52966.
3. Wang, B.; Liu, H.; Zhang, B.; Han, Y.; Shen, C.; Lin, Q.; Chen, H. Development of antibacterial and high light transmittance bulk materials: Incorporation and sustained release of hydrophobic or hydrophilic antibiotics. Colloids and Surfaces B: *Biointerfaces*, **2016**, *141*, 483-490.
4. Lee, J.H.; Oh, J.W.; Nam, S.H.; Cha, Y.S.; Kim, G.H.; Rhim, W.K.; Kim, N.H.; Kim, S.W.; Han, S.W.; Suh, Y.D; Nam, J.M. Synthesis, Optical Properties, and Multiplexed Raman Bio-Imaging of Surface Roughness-Controlled Nanobridged Nanogap Particles. *Small*, **2016**, *12(34)*, 4726-4734.
5. Behrooz, A.; Waterman, P.; Vasquez, K.O.; Meganck, J.; Peterson, J.D.; Faqir, I.; Kempner, J. Multispectral open-air intraoperative fluorescence imaging. *Opt Lett*, **2017**, *42(15)*, 2964-2967.
6. Lee, O.; Kim, J.; Park, G.; Kim, M.; Son, S.; Ha, S.; Oh, C. Non-invasive assessment of cutaneous wound healing using fluorescent

imaging. *Skin Res Tech*, **2015**, *21(1)*, 108-113.

7. Yan, K.; Guo, Q.; Wu, F.; Sun, J.; Zhao, H.; Kwok, H. S. Polarization-independent nematic liquid crystal phase modulator based on optical compensation with sub-millisecond response. Optics express, 2019, 27(7), 9925-9932.